

Single-photon ionization in intense, fluctuating pulses

Sajal Kumar Giri, Ulf Saalmann  and Jan M. Rost

Max-Planck-Institute for the Physics of Complex Systems, Dresden, Germany

ABSTRACT

High intensities in laser–matter interaction drive nonlinear processes. Whereas at low frequencies thereby multi-photon absorption and above-threshold ionization emerges, in the case of high frequencies single-photon absorption remains prevailing. However, multiple absorption and emission of photons renders this single-photon ionization sensitive to energy and shape of the laser pulse. This becomes relevant for intense, fluctuating pulses as generated in existing and upcoming free-electron laser sources. We study their effect on the ionization of a model atom numerically and formulate suitable parameters to characterize the evolution from the linear response at low intensity to the intricate dynamics at high intensities.

ARTICLE HISTORY

Received 22 September 2016
Accepted 28 November 2016

KEYWORDS

Photo-effect; strong-field ionization; free-electron lasers; partial-coherence method

1. Introduction

The interaction of photons with matter is one of a few fundamental mechanisms to obtain detailed knowledge about matter. The photo-effect explains quantum mechanically, how this interaction works in the linear, i.e. weak coupling regime, where single-photon processes dominate. The electrons set free by the photo-effect are well described by a perturbative treatment of the matter–light dynamics (1) and the resulting photo-electron spectrum for electrons with initial energy E_0 reads (we will use atomic units throughout the paper unless specified otherwise)

$$S(E) = \left| d(E) \int dt A(t) e^{-i[E_0 - E]t} \right|^2$$
$$\text{with } d(E) \equiv \sum_{\alpha} \langle \varphi_{\alpha}(E) | \hat{p} | \varphi_0 \rangle, \quad (1)$$

where $A(t)$ is the time-dependent vector potential of the laser pulse and the index α denotes all degenerate states at energy E . Of course, some matrix elements in the sum may vanish because of selection rules.

In this contribution we study stochastic or fluctuating (both terms are used synonymously throughout) laser pulses. In particular, we consider pulses with a possibly short, but finite coherence time, which induce an unitary electron dynamics. The photo-effect as described by (1) remains valid for such laser pulses, as long as the condition for single-photon processes persists, rendering a correlation between the photons irrelevant for the photo-ionization process. Formally, this is reflected by

the fact that in Equation (1) the light neither influences the sum of dipole matrix elements $d(E)$ nor the initial and final energies E_0 and E of the electron. For intense laser pulses, however, nonlinear photon–electron interactions must be considered beyond the linear response of (1) through which stochastic pulses can influence photo-ionization. Above-threshold ionization, as known from the low-frequency regime (2), is very unlikely (3) mainly due to the tiny continuum–continuum matrix elements.

The advent of free-electron lasers (FELs) producing intense pulses in the high frequency regime (4–6) with ever shorter pulse durations (7–10) has given a new incentive to understand the interplay of nonlinear light–matter coupling and stochastic pulses, since the FELs create light through self-amplified spontaneous emission (SASE) with considerable shot-to-shot fluctuations in the pulse shape (11). At a first glance, one may think that the applicability of (1) prevails: Single-photon ionization is by far the dominating process as dipole matrix elements in the continuum are weak compared to those elements involving bound states. Yet, this does not prevent nonlinear (multiple) photon coupling which is realized by virtual emission and absorption of several photons, altering the states φ involved in (1) and their energies.

As a consequence, high frequency intense stochastic pulses may influence considerably single-photon ionization (12, 13). To study their influence systematically is the subject of this work. We will present numerically obtained ionization probabilities for a hydrogenic model atom exposed to stochastic FEL pulses which we generate with the partial-coherence method (14), which has been

tested experimentally by measuring the second-order autocorrelation of SASE pulses at SCSS (15). The impact of the stochasticity was pointed out a long time ago (16–18) mainly in connection with multi-photon processes.

2. Theoretical model

In order to facilitate a systematic treatment we use the well established soft-core 1d model atom with a modified Coulomb potential

$$\hat{H} = -\frac{1}{2} \frac{\partial^2}{\partial x^2} + V(x) + A(t) i \frac{\partial}{\partial x}, \quad (2a)$$

$$V(x) = -\frac{1}{\sqrt{x^2 + s}}. \quad (2b)$$

With the choice of $s = 2$ the ground-state energy in the potential (2b) matches the one of hydrogen $E_0 = -1/2$.

The partial-coherence method (14) for stochastic pulses proceeds from a Gaussian pulse for the vector potential

$$A(t) = A_* G(t) g(t) \cos(\omega t) \quad (3a)$$

$$G(t) = \exp(-\ln 2 [t/T]^2), \quad (3b)$$

$$g(t) = \exp(-\ln 2 [t/\tau]^2), \quad (3c)$$

with amplitude A_* and carrier frequency ω . The two Gaussian envelope functions with respective widths T and τ serve different purposes. Whereas $G(t)$ will be used as masking function in time and thus fixes the typical pulse duration T , Gaussian $g(t)$ characterizes the time scale of the fluctuations by means of the coherence time τ . Thus $\tau \ll T$ (or $\tau \gg T$) implies strongly (or weakly) fluctuating pulses.

For solving the time-dependent Schrödinger equation by means of a Crank–Nicolson propagator we need the pulse at certain time instances t_k ,

$$A_k = A(t_k) = A_* G(t_k) g(t_k) \cos(\omega t_k), \quad (4)$$

with k (and all other indices used below) running from $-n$ to $+n$. We use an equidistant grid of times $t_k = k \cdot \delta t$ with arguments in square brackets $[\xi_l]$ denoting $(\xi_{-n}, \xi_{-n+1}, \dots, \xi_{+n})$. The partial coherence method generates the stochastic pulse according to

$$\tilde{A}_k[\phi_l] \equiv A_* G(t_k) \mathcal{F}^{-1} \left[e^{i\phi_l} \mathcal{F} [g(t_k) \cos(\omega t_k)] \right], \quad (5)$$

with a complete set of random phases $[\phi_l]$ uniformly distributed in the range $-\pi \dots +\pi$. In Equation (5) \mathcal{F} and \mathcal{F}^{-1} are discrete forward and backward Fourier transforms (FT), i.e. $y_l = \mathcal{F}[x_k]$ means $y_l = \sum_k e^{i\omega_l t_k} x_k$. In order to make the pulse real we apply the constraint

$\phi_{-l} = -\phi_{+l}$ for all l . One easily obtains from (5) that $\tilde{A}_k = A_k$ holds in (4) if $\phi_l = 0$ for all l . In other words, for identical phases and identical times T and τ we get the original Gaussian pulse (4) back. Note, that an overall phase defines the carrier-envelope phase, which is irrelevant for the many-cycle pulses we consider here.

The pulse constructed according to (5) was shown (14) to give approximately a Gamma distribution of pulse energies

$$P[\phi_l] = \frac{1}{4 \delta t} \sum_k |\tilde{A}_{k+1}[\phi_l] - \tilde{A}_{k-1}[\phi_l]|^2, \quad (6)$$

which is characterized by the average pulse energy \bar{P} and has a single maximum P_{\max} . This maximal pulse energy is realized by the original (deterministic) Gaussian (4). For any other set of phases the pulse energy P is smaller.

In what is presented below, the system is discretized for $x = -200 \dots +200$ with 2000 steps of width $\delta x = 0.2$. As time step we use $\delta t = 5.722 \times 10^{-3}$ and $n = 2^{19}$. The carrier frequency is $\omega = 3/2$.

3. From perturbative to non-perturbative stochastic pulses

In the following, we present systematic numerical results for ionization by stochastic pulses as a function of pulse energy P . The six (3×2) different parameter sets cover the transition from the perturbative regime of the photo-effect (1) to the nonlinear regime for which we have solved the Schrödinger equation with the Hamilton operator (2) at two fluctuation scenarios with $\tau = T/10$ and $\tau = T$, respectively.

We define the pre-factor A_* as

$$A_* = \frac{1}{\omega} \sqrt{\frac{P_{\max}}{\bar{P}} \sqrt{\frac{1 + [T/\tau]^2}{2}} \frac{I_{\bar{P}}}{I_0}} \quad \text{with } I_0 = 3.51 \times 10^{16} \text{ W/cm}^2, \quad (7)$$

which implies that pulses with $P = \bar{P}$ have a given intensity of $I_{\bar{P}}$. To show the transition from perturbative to non-perturbative behaviour we present results for the three cases $I_{\bar{P}} = 2 \times 10^{16}, 2 \times 10^{17}$ and $2 \times 10^{18} \text{ W/cm}^2$.

As Figure 1 illustrates, a given pulse energy P has different implications for the ionization dynamics depending on the strength of the pulse. For a ‘weak’ pulse (Figures 1(a) and (d)) the results can be understood in the framework of the photo-effect, cf. Equation (1). In this case the ionization probability depends linearly on the pulse energy as one would expect from perturbation theory, represented by the grey line in Figure 1(a). Stronger fluctuations (Figure 1(a)) broaden the distribution around

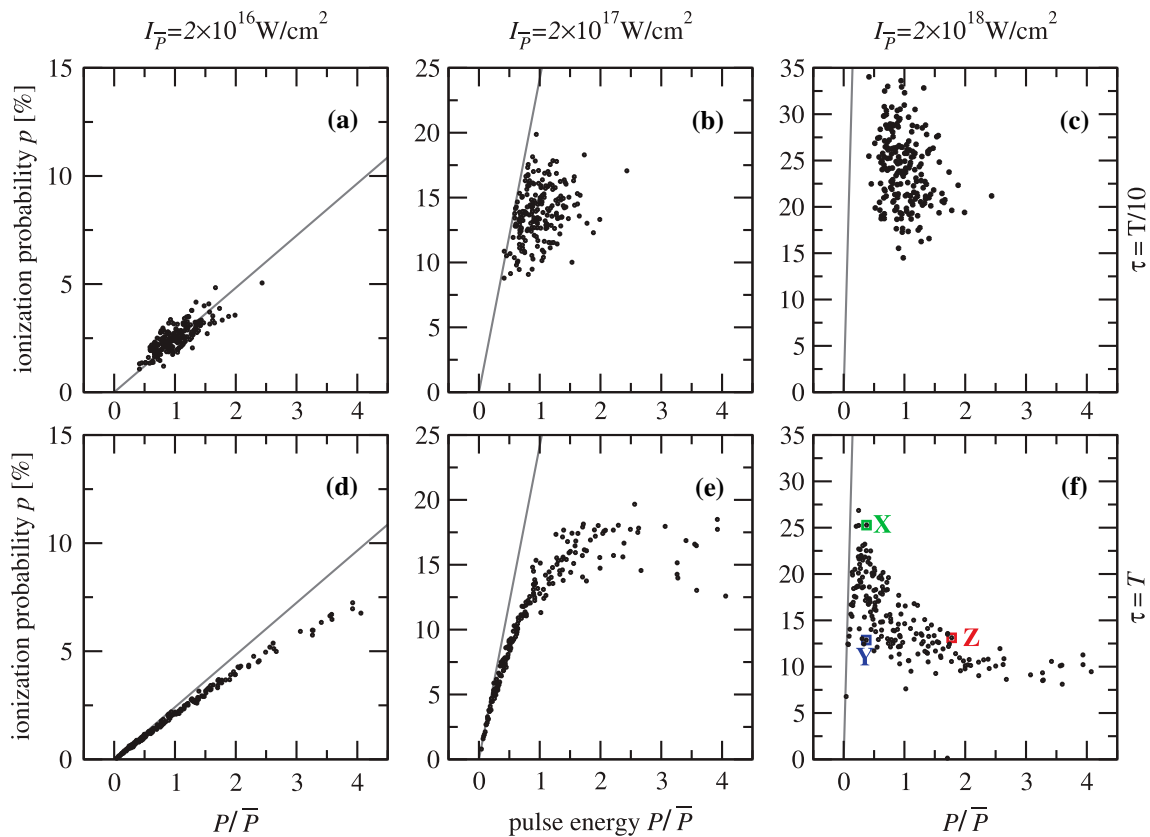


Figure 1. Ionization probability for six sets of 200 pulses each with $T = 1$ fs and $\omega = 3/2$. The time scale for the fluctuations is $\tau = T/10$ (upper row) and $\tau = T$ (lower row), respectively. The intensity I increases from left to right. The prediction from perturbation theory (1) is shown by the grey lines. The three pulses X, Y and Z from the lower right panel are studied in detail below.

the lines since the larger bandwidth uncovers the strong energy dependence of the matrix elements $d(E)$ in the photo-electron spectrum. For larger τ (Figure 1(d)) the distribution is much narrower and follows the perturbative line. For high pulse energies $P > 3\bar{P}$, the ionization yields deviate slightly from the perturbative one towards lower probabilities p .

This deviation becomes more pronounced in the 2nd set with $I_{\bar{P}} = 2 \times 10^{17}$ W/cm² shown in Figure 1(b) and (e). For even higher intensity $I_{\bar{P}} = 2 \times 10^{18}$ W/cm² shown in Figures 1(c) and (f), the ionization yield assumes a shape, qualitatively different from the perturbative result. Indeed, one sees the effect of stabilization (19, 20), i.e. that pulses with a higher pulse energy P result in a lower ionization probability p . The fact, that p hardly exceeds 25%, is due to the rather short pulse duration of $T = 1$ fs that was employed.

4. The effect of individual shapes for strongly fluctuating pulses

In order to understand the behaviour in the case of large fluctuations of FEL pulses we will consider three

individual pulses in more detail. These pulses are marked in Figure 1(f) by coloured squares and letters X, Y and Z. We have chosen the three pulses such that $P_X \approx P_Y$ and such that $p_Y \approx p_Z$. Although the pulse energies for X and Y are approximately the same ($P \approx 0.37\bar{P}$), the ionization probabilities differ by as much as a factor of 2 ($p_X \approx 25\%$, $p_Y \approx 13\%$). On the other hand, the two pulses Y and Z differ in their pulse energy by a factor larger than 4 ($P_Y \approx 0.37\bar{P}$, $P_Z \approx 1.69\bar{P}$), but both induce a similar ionization probability of $p \approx 13\%$.

The upper row of Figure 2 shows the three pulses in the time domain. Apparently, pulse Z resembles most closely the original Gaussian pulse. That is the reason that it has the largest pulse energy, which can be also seen from the FT in the 2nd row of Figure 2. It covers not only the largest area but also looks like a Gaussian, whereas the other two pulses (X and Y) show a bimodal FT.

Most interestingly—and in strong contrast to perturbation theory—the photo-electron spectra (shown in the 3rd row of Figure 2) differ considerably from the FTs of the pulses. This cannot be explained by the energy dependence of the matrix elements $d(E)$. Rather, effects like stabilization (19, 20) and dynamic interference

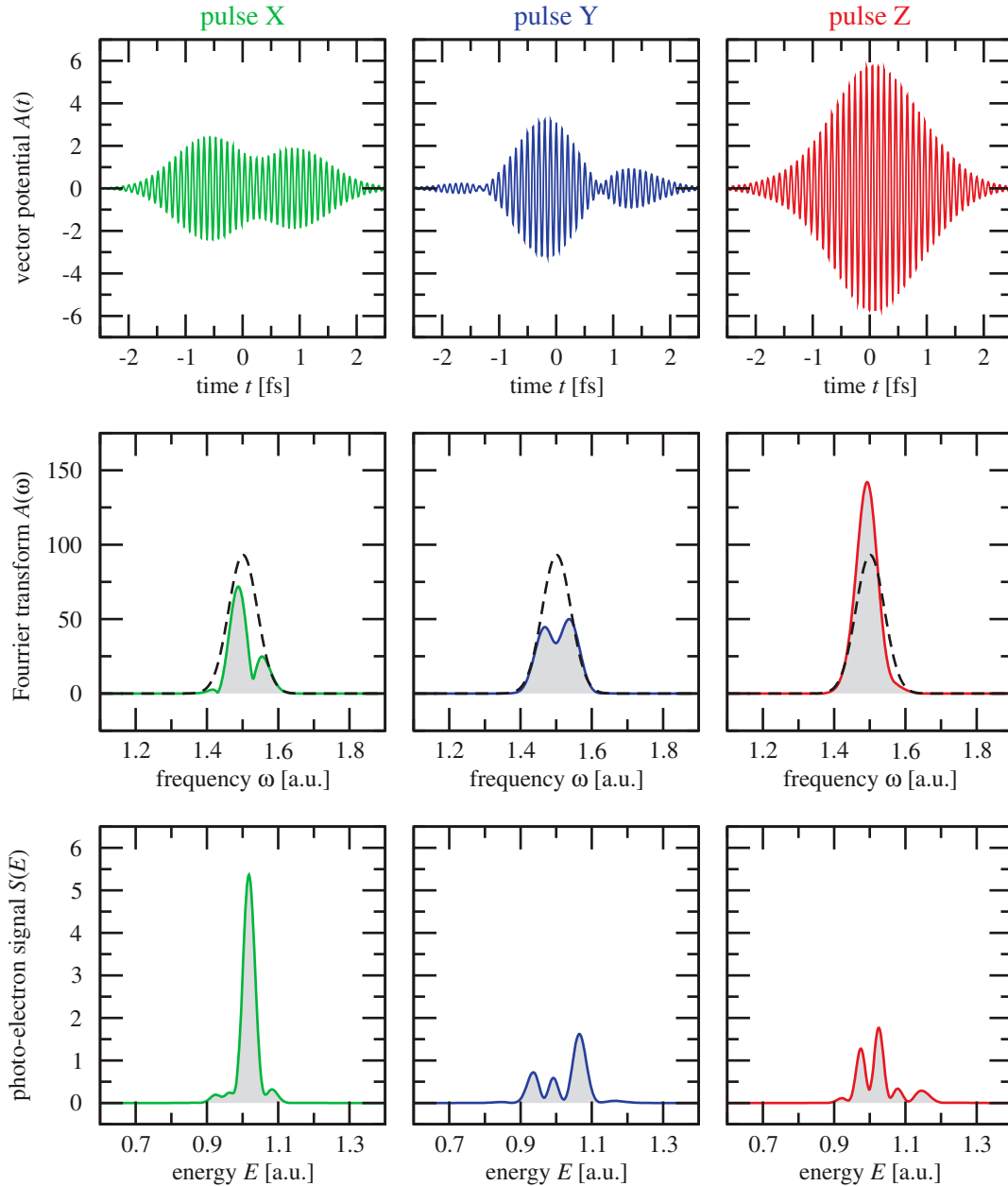


Figure 2. Details for the three pulses specified in Figure 1 with X, Y and Z, respectively. Upper row: time-dependent vector potential $A(t)$, middle row: FT $A(\omega)$ in comparison to a Gaussian pulse (dashed line), lower row: photo-electron signal $S(E)$.

(21, 22) are responsible for the multi-peak structure and the overall ionization probability. Typically, these effects are strongest if the maximal vector potential is large, here for Y and particular for Z. Conversely, an overall small vector potential will produce spectra with a large single-peak as in the case X. One may quantify this observation with the pulse length, that fluctuates from pulse to pulse and can be calculated as

$$\tilde{T} \equiv \sqrt{8 \ln 2 \frac{\int dt t^2 A^2(t)}{\int dt A^2(t)}}. \quad (8)$$

With this definition we get for the original Gaussian pulse $\tilde{T} = 1$ fs and for our three pulses $\tilde{T}_X = 1.97$ fs, $\tilde{T}_Y = 1.23$ fs and $\tilde{T}_Z = 1.36$ fs, respectively. All pulses are longer than the Fourier limit with X almost twice as long. Pulse Y is about 1/3 shorter but since it has the same energy it is considerably stronger, which brings it into the stabilization regime and explains the strongly reduced ionization probability.

To demonstrate the intricate interplay of pulse shape and pulse energy in the nonlinear single-photon ionization regime, we finally present results, which can only be obtained theoretically: We follow the ionization yield as

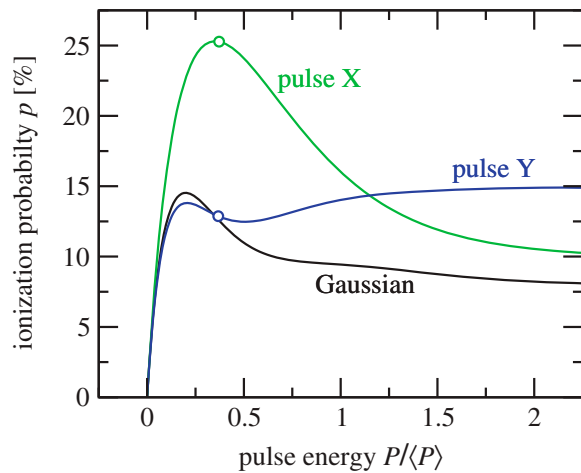


Figure 3. Ionization probability for the two pulses specified in Figure 1 with X and Y. We fixed the (randomly chosen) phases and varied the pulse energy by changing the pre-factor A_* in Equation (5). For comparison we show the result for Gaussian pulse as well. The circles mark the pulses shown in Figure 1.

a function of pulse energy for a single given pulse shape (fixed set of randomly chosen phase parameters $[\phi_l]$). This is done in Figure 3 for the two pulses X and Y as a function of the pulse energy by varying the pre-factor (7). Additionally we show the corresponding ionization probability for a Gaussian pulse. For low pulse energies $P < 0.1\bar{P}$ one sees the same linear response in all three cases. Deviations occur at around $P \approx 0.2\bar{P}$ but to a very different extent. As already shown in Figure 1 for $P \approx 0.37\bar{P}$ the ionization probability differs by a factor of 2. While pulse X behaves for higher energies P qualitatively as the Gaussian pulse with a slow decay after the maximum, p for pulse Y only falls off briefly only to increase afterwards. This leads to the interesting observation that Y becomes more efficient in ionizing the system than X for higher pulse energy.

5. Conclusions

We have explored the interplay of fluctuations and pulse strength in the regime of high photon frequencies relevant for single-photon ionization. For the ionization probability as a function of pulse energy $p(P)$, we find a gradual deviation from the perturbative (linear) increase with increasing intensity for the mean energy. Eventually, $p(P)$ qualitatively changes its shape at high intensities and exhibits a large spread revealing a sensitive dependence on individual pulse shapes. This behaviour reveals consequences of dynamical effects which have been identified in deterministic pulses, such as stabilization and dynamic interference. They lead to ionization probabilities which can differ significantly for two pulses of the same energy. In future work it may be possible to characterize

the spread of the ionization probability as a function of pulse energy quantitatively using the properties of the deterministic dynamical effects.

Disclosure statement

No potential conflict of interest was reported by the authors.

Funding

This work has been supported by the Deutsche Forschungsgemeinschaft (DFG) through the priority programme 1840 ‘Quantum Dynamics in Tailored Intense Fields’.

ORCID

Ulf Saalmann  <http://orcid.org/0000-0003-3208-8273>

References

- (1) Bransden, B.H.; Joachain, C.J. *Physics of Atoms and Molecules*; Edinburgh, Pearson Education Limited, 2003.
- (2) Agostini, P.; Fabre, F.; Mainfray, G.; Petite, G.; Rahman, N.K. *Phys. Rev. Lett.* **1979**, *42*, 1127–1130.
- (3) Bachau, H.; Budrigo, O.; Dondera, M.; Florescu, V. *Cent. Eur. J. Phys.* **2012**, *11* (Oct), 1091–1098.
- (4) Ackermann, W.; Asova, G.; Ayzvayan, V.; Azima, A.; Baboi, N.; Bähr, J.; Balandin, V.; Beutner, B.; Brandt, A.; Bolzmann, A.; Brinkmann, R.; Brovko, O.I.; Castellano, M.; Castro, P.; Catani, L.; Chiadroni, E.; Choroba, S.; Cianchi, A.; Costello, J.T.; Cubaynes, D.; Dardis, J.; Decking, W.; Delsim-Hashemi, H.; Delserieys, A.; Pirro, D.G.; Dohlus, M.; Düsterer, S.; Eckhardt, A.; Edwards, H.T.; Faatz, B.; Feldhaus, J.; Flöttmann, K.; Frisch, J.; Fröhlich, L.; Garvey, T.; Gensch, U.; Gerth, C.H.; Görler, M.; Golubeva, N.; Grabosch, H.-J.; Grecki, M.; Grimm, O.; Hacker, K.; Hahn, U.; Han, J.H.; Honkavaara, K.; Hott, T.; Hüning, M.; Ivanisenko, Y.; Jaeschke, E.; Jalmuzna, W.; Jezynski, T.; Kammering, R.; Katalov, V.; Kavanagh, K.; Kennedy, E.T.; Khodyachykh, S.; Klose, K.; Kocharyan, V.; Körfer, M.; Kollwe, M.; Koprek, W.; Korepanov, S.; Kostin, D.; Krassilnikov, M.; Kube, G.; Kuhlmann, M.; Lewis C.L.S.; Lilje, L.; Limberg, T.; Lipka, D.; Löhl, F.; Luna, H.; Luong, M.; Martins, M.; Meyer, M.; Michelato, P.; Miltchev, V.; Möller, W.D.; Monaco, L.; Müller, W.F.O.; Napieralski, O.; Napoly, O.; Nicolosi, P.; Nölle, D.; Nuñez, T.; Oppelt, A.; Pagani, C.; Paparella, R.; Pchalek, N.; Pedregosa-Gutierrez, J.; Petersen, B.; Petrosyan, B.; Petrosyan, G.; Petrosyan, L.; Pflüger, J.; Plönjes, E.; Poletto, L.; Pozniak, K.; Prat, E.; Proch, D.; Pucyk, P.; Radcliffe, P.; Redlin, H.; Rehlich, K.; Richter, M.; Roehrs, M.; Roensch, J.; Romaniuk, K.; Ross, M.; Rossbach, J.; Rybnikov, V.; Sachwitz, M.; Saldin, E.L.; Sandner, W.; Schlarb, H.; Schmidt, B.; Schmitz, M.; Schmüser, P.; Schneider, J.R.; Schneidmiller, E.A.; Schnepf, S.; Schreiber, S.; Seidel, M.; Sertore, D.; Shabunov, A.V.; Simon, C.; Simrock, S.; Sombrowski, E.; Sorokin, A.A.; Spanknebel, P.; Spesyvtsev, R.; Staykov, L.; Steffen, B.; Stephan, F.; Stulle, F.; Thom, H.; Tiedtke, K.

- Tischer, M.; Toleikis, S.; Treusch, R.; Trines, D.; Tsakov, I.; Vogel, E.; Weiland, T.; Weise, H.; Wellhöfer, M.; Wendt, M.; Will, I.; Winter, A.; Wittenburg, K.; Wurth, W.; Yeates, P.; Yurkov, M.V.; Zagorodnov, I.; Zapfe, K. *Nat. Photon.* **2007**, *1*, 336–342.
- (5) Emma, P.; Akre, R.; Arthur, J.; Bionta, R.; Bostedt, C.; Bozek, J.; Brachmann, A.; Bucksbaum, P.; Coffee, R.; Decker, F.-J.; Ding, Y.; Dowell, D.; Edstrom, S.; Fisher, A.; Frisch, J.; Gilevich, A.; Hastings, J.; Hays, G.; Hering, P.; Huang, Z.; Iverson, R.; Loos, H.; Messerschmidt, M.; Miahnahri, A.; Moeller, S.; Nuhn, H.-D.; Pile, G.; Ratner, D.; Rzepiela, J.; Schultz, D.; Smith, T.; Stefan, P.; Tompkins, H.; Turner, J.; Welch, J.; White, W.; Wu, J.; Yocky, G.; Galayda, J. *Nat. Photon.* **2010**, *4*, 641–647.
- (6) McNeil, B.W.J.; Thompson, N.R. *Nat. Photon.* **2010**, *4* (Dec), 814–821.
- (7) Emma, P.; Bane, K.; Cornacchia, M.; Huang, Z.; Schlarb, H.; Stupakov, G.; Walz, D. *Phys. Rev. Lett.* **2004**, *92* (Feb), 074801.
- (8) Zholents, A.A.; Fawley, W.M. *Phys. Rev. Lett.* **2004**, *92* (Jun), 224801-1–224801-4.
- (9) Saldin, E.L.; Schneidmiller, E.A.; Yurkov, M.V. *Phys. Rev. ST Accel. Beams* **2006**, *9* (May), 050702.
- (10) Sadler, J.D.; Nathvani, R.; Oleśkiewicz, P.; Ceurvorst, L.A.; Ratan, N.; Kasim, M.F.; Trines, R.M.G.M.; Bingham, R.; Norreys, P.A. *Sci. Rep.* **2015**, *5* (Nov), 16755-1–16755-7.
- (11) Saldin, E.L.; Schneidmiller, E.A.; Yurkov, M.V. *Opt. Commun.* **2008**, *281* (Mar), 1179–1188.
- (12) Rohringer, N.; Santra, R. *Phys. Rev. A* **2007**, *76* (Sep), 033416.
- (13) Nikolopoulos, G.M.; Lambropoulos, P. *Phys. Rev. A* **2012**, *86* (Sep), 033420.
- (14) Pfeifer, T.; Jiang, Y.; Düsterer, S.; Moshhammer, R.; Ullrich, J. *Opt. Lett.* **2010**, *35* (Oct), 3441–3443.
- (15) Moshhammer, R.; Pfeifer, Th.; Rudenko, A.; Jiang, Y.H.; Foucar, L.; Kurka, M.; Kühnel, K.U.; Schröter, C.D.; Ullrich, J.; Herrwerth, O.; Kling, M.F.; Liu, X.-J.; Motomura, K.; Fukuzawa, H.; Yamada, A.; Ueda, K.; Ishikawa, K.L.; Nagaya, K.; Iwayama, H.; Sugishima, A.; Mizoguchi, Y.; Yase, S.; Yao, M.; Saito, N.; Belkacem, A.; Nagasono, M.; Higashiya, A.; Yabashi, M.; Ishikawa, T.; Ohashi, H.; Kimura, H.; Togashi, T. *Opt. Express* **2011**, *19* (Oct), 21698–21706.
- (16) Lambropoulos, P.; Kikuchi, C.; Osborn, R.K. *Phys. Rev.* **1966**, *1081* (Apr), 144–1086.
- (17) Mollow, B.R. *Phys. Rev.* **1968**, *175* (Nov), 1555–1563.
- (18) Agarwal, G.S. *Phys. Rev. A* **1970**, *1*, 1445–1459.
- (19) Gavrilin, M. *J. Phys. B* **2002**, *35* (Sep), R147.
- (20) Popov, A.M.; Tikhonova, O.V.; Volkova, E.A. *J. Phys. B* **2003**, *36* (May), R125.
- (21) Toyota, K.; Tolstikhin, O.I.; Morishita, T.; Watanabe, S. *Phys. Rev. A* **2007**, *76* (Oct), 043418.
- (22) Demekhin, P.V.; Cederbaum, L.S. *Phys. Rev. Lett.* **2012**, *108* (Jun), 253001-1–253001-5.